Contribution No. 7200 from the Arthur Amos Noyes Laboratory, California Institute of Technology, Pasadena, California 91125

# Hexanuclear Tungsten Cluster Structures: $W_6Cl_{14}^{2-}$, $W_6Br_{14}^{2-}$, and $W_6I_{14}^{2-}$. Relevance to Unusual Emissive Behavior

Thomas C. Zietlow, William P. Schaefer, Behzad Sadeghi, Nhi Hua, and Harry B. Gray*

*Received May 30, 1985*

The compounds $[(n\text{-}C_4H_9)_4N]_2W_6X_{14}$ (X = Cl, Br, I) crystallize with $Z = 2$ in space group $P2_1/n$ with the following cell dimensions: $a$ = 18.512 (3) [Cl], 18.968 (8) [Br], 11.553 (1) Å [I]; $b$ = 11.661 (1) [Cl], 11.913 (6) [Br], 11.486 (3) Å [I]; $c$ = 12.789 (1) [Cl], 13.263 (6) [Br], 24.554 (13) Å [I]; $\beta$ = 90.17 (1) [Cl], 90.87 (4) [Br], 96.77 (4)° [I]. The Cl and Br compounds are isostructural. The tungsten clusters are nearly perfect octahedra, although octahedral symmetry is not imposed crystallographically. The metal–halide bond distances do not vary simply with ionic radii for the three structures. The structural studies confirm the trend established by spectroscopic data, that the $\mu_3$-halides interact more strongly with the tungsten atoms in the $W_6I_{14}^{2-}$ cluster than in $W_6Cl_{14}^{2-}$. The tungsten–tungsten bonds are longer in $W_6I_{14}^{2-}$ than in $W_6Cl_{14}^{2-}$, thereby implying that the overlap of the tungsten orbitals is not the sole factor in the ordering of excited-state energies. Metal back-bonding to X is suggested as an explanation of the emission energy trends in the $W_6X_{14}^{2-}$ clusters.

Studies of the photophysical behavior of the hexanuclear clusters $M_6X_{14}^{2-}$ (M = Mo, W; X = Cl, Br, I) have suggested that the emissive excited state of $Mo_6X_{14}^{2-}$ is metal-centered.[1,2] Both the energy of the emissive state and the radiative decay rate are invariant upon exchange of the halide. The temperature dependence of the excited-state lifetime shows that the three molybdenum clusters, $Mo_6Cl_{14}^{2-}$, $Mo_6Br_{14}^{2-}$, and $Mo_6I_{14}^{2-}$, differ only in their nonradiative decay rates, with the largest $k_{nr}$ associated with iodide, which is the ligand that is the most polarizable and interactive with the solvent.[3]

The tungsten series, $W_6X_{14}^{2-}$, presents a different picture of the emissive state. The excited-state energy is halide-dependent: $W_6Cl_{14}^{2-}$ (1.83 eV) < $W_6Br_{14}^{2-}$ (1.85 eV) < $W_6I_{14}^{2-}$ (2.05 eV), which is the *opposite* order from that expected by incorporation of some ligand-to-metal charge-transfer character into the transition.[4] From previous work done on the tungsten clusters, it is known that the energy of the emissive state is determined mainly by the inner core of triply bridging halides, with the terminal halides playing a minor role. (The small terminal halide effect diminishes as the triply bridging halide is changed from chloride to bromide to iodide.) The outer halides do influence the nonradiative decay rate, but their effect on the radiative rate is very small.[5]

Because we would like to elucidate the relative degrees of metal–metal and metal–halide interactions as the halide is varied, we have determined the ground-state structures of the three tungsten clusters. These results (X-ray structures of $[(n\text{-}C_4H_9)_4N]_2W_6Cl_{14}$, $[(n\text{-}C_4H_9)_4N]_2W_6Br_{14}$, and $[(n\text{-}C_4H_9)_4N]_2W_6I_{14}$) and their relevance to emission properties are reported herein.

## Experimental Section

The complexes were synthesized as described previously;[6] they were crystallized by layering petroleum ether on a methylene chloride solution of the cluster.

**X-ray Structures.** All scattering factors (W, I, Br, Cl, C, H, N) were taken from ref 7.

**$[(n\text{-}C_4H_9)_4N]_2W_6Cl_{14}$.** A crystal with dimensions 0.24 × 0.24 × 0.17 mm was mounted on a glass fiber. The crystal was then centered on a CAD4 diffractometer equipped with graphite-monochromated Mo Kα radiation for intensity data collection. Unit cell dimensions were obtained from the setting angles of 25 reflections with 25° < 2θ < 31°. Space group $P2_1/n$, a special setting of No. 14, was chosen on the basis of the systematic absences $h0l$, $h + l = 2n + 1$, and $0k0$, $k = 2n + 1$, in the intensity data. This space group has four equivalent positions, $\pm(x, y, z; {}^1/_2 - x, {}^1/_2 + y, {}^1/_2 - z)$. Two sets of data were collected with a total of 10 766 reflections in the quadrants $\pm h,k,l$ and $\pm h,-k,l$. Crystal data are collected in Table I. After every 10 000 s of X-ray exposure, three check reflections were monitored to check crystal decay; they showed no variations greater than those expected statistically. The data were corrected for absorption by Gaussian integration over an 8 × 8 × 8 grid; transmission factors varied from 0.081 to 0.172. After being corrected for background, the two data sets were merged to give 4858 independent reflections, which were all used in the structure solution and refinement. Variances were assigned to individual reflections on the basis of counting statistics plus as additional term, $(0.014I)^2$, to account for intensity-dependent errors. Final variances were assigned by standard propagation of error plus an additional term, $(0.014\bar{I})^2$.

**Table I.** Crystal Data for $[(n\text{-}C_4H_9)_4N]_2W_6X_{14}$[a]

| | X | | |
|---|---|---|---|
| | Cl | Br | I |
| fw | 2096.55 | 2692.76 | 3364.71 |
| $a$, Å | 18.512 (3) | 18.968 (8) | 11.553 (7) |
| $b$, Å | 11.661 (1) | 11.913 (6) | 11.486 (3) |
| $c$, Å | 12.789 (1) | 13.263 (6) | 24.554 (13) |
| $\beta$, deg | 90.17 (4) | 90.87 (4) | 96.77 (4) |
| $V$, Å$^3$ | 2760 (1) | 2997 (1) | 3235 (3) |
| $\mu$, cm$^{-1}$ | 134.39 | 220.35 | 179.96 |
| $F(000)$, e | 960 | 1205 | 2518 |
| $d_x$, g cm$^{-3}$ | 2.52 | 2.98 | 3.45 |

[a] Space group $P2_1/n$ (No. 14); $T$ = 21 °C; λ(Mo Kα) = 0.710 73 Å.

The anions are located at a center of symmetry in the unit cell. Interpretation of Patterson maps gave the positions of the three tungsten atoms. From structure factor–Fourier calculations the seven chlorine atoms and the non-hydrogen atoms in the cation were located. The positions of the hydrogen atoms were calculated from known geometry and assumed staggered conformations. The tungsten and chlorine atoms were given anisotropic thermal parameters while the atoms in the cation were given isotropic thermal parameters. Several cycles of least-squares refinement led to convergence with $R$ of 0.062 for 4157 data. For the strong data with $F_o^2 > 3\sigma F_o^2$, $R$ = 0.053 for 3519 reflections. The goodness of fit $(=[\sum w(F_o^2 - F_c^2)^2/(n-p)]^{1/2})$ is 2.72 for $n$ = 4858 reflections and $p$ = 160 parameters (6 strong low-angle reflections were given zero weight in this refinement). Final parameters are in Table II,[8] and bond lengths are in Table III.

**$[(n\text{-}C_4H_9)_4N]_2W_6Br_{14}$.** Preliminary photographs showed a monoclinic cell with systematic absences indicating space group $P2_1/n$. An irregularly shaped crystal with dimensions 0.17 × 0.13 × 0.15 mm was carefully centered on a Nicolet $P2_1$ diffractometer. Unit cell dimensions were obtained by least-squares fit to setting angles of 15 reflections with 20° < 2θ < 26°. Crystal data are given in Table I. A total of 11 386 reflections with 2θ < 55° in the quadrants $h,\pm k,\pm l$ were measured with θ–2θ scans of 2° plus dispersion at a scan speed in 2θ of 2 or 4°/min. Three check reflections were monitored every 97 reflections and showed no changes greater than those expected from counting statistics. The data were corrected for absorption by Gaussian integration, and Lorentz

(1) Maverick, A. W.; Gray, H. B. *J. Am. Chem. Soc.* **1981**, *103*, 1298.
(2) Maverick, A. W.; Najdzionek, J. S.; MacKenzie, D.; Nocera, D. G.; Gray, H. B. *J. Am. Chem. Soc.* **1983**, *105*, 1878.
(3) Zietlow, T. C.; Gray, H. B., unpublished results.
(4) Zietlow, T. C.; Hopkins, M. D.; Gray, H. B. *J. Solid State Chem.* **1985**, *57*, 112.
(5) Zietlow, T. C.; Nocera, D. G.; Gray, H. B. *Inorg. Chem.*, in press.
(6) Hogue, R. D.; McCarley, R. E. *Inorg. Chem.* **1970**, *9*, 1355.
(7) *International Tables for X-ray Crystallography*; Kynoch: Birmingham, England, 1974; Vol. IV, p 72.

(8) Definition:

$$U_{eq} = {}^1/_3[\sum_i\sum_j U_{ij}(a_i^* a_j^*)(\bar{a}_i\bar{a}_j)] \qquad \sigma(U_{eq}) = \frac{1}{6^{1/2}}\left\langle\frac{\sigma U_{ii}}{U_{ii}}\right\rangle U_{eq}$$

0020-1669/86/1325-2195$01.50/0 

**Table II.** Final Parameters for $[(n\text{-}C_4H_9)_4N]_2W_6Cl_{14}$[a]

| atom | x | y | z | $U_{eq}$ or B, Å$^2$ |
|---|---|---|---|---|
| W(1) | 1950 (3) | 5404 (5) | 86765 (4) | 382 (1) |
| W(2) | 8474 (3) | 6377 (5) | 4864 (4) | 366 (1) |
| W(3) | 95159 (3) | 13395 (5) | 3083 (4) | 375 (1) |
| Cl(1) | 19573 (19) | 14551 (36) | 11428 (32) | 611 (10) |
| Cl(2) | 5370 (18) | 24154 (31) | 94870 (28) | 493 (8) |
| Cl(3) | 89152 (17) | 12032 (30) | 85570 (25) | 431 (8) |
| Cl(4) | 85386 (17) | 1315 (32) | 10897 (26) | 462 (8) |
| Cl(5) | 1633 (19) | 13882 (33) | 20225 (26) | 502 (9) |
| Cl(6) | 38721 (22) | 19270 (38) | 57539 (36) | 711 (12) |
| Cl(7) | 4343 (23) | 11956 (45) | 69167 (30) | 768 (13) |
| N(1) | 2087 (7) | −249 (10) | 4750 (9) | 4.2 (3) |
| C(1) | 1369 (9) | −882 (15) | 4818 (14) | 5.5 (4) |
| C(2) | 1390 (13) | −2114 (20) | 4745 (18) | 8.6 (6) |
| C(3) | 710 (14) | −2675 (25) | 5214 (21) | 9.7 (7) |
| C(4) | 714 (26) | −3773 (43) | 5345 (36) | 22 (2) |
| C(5) | 2391 (9) | −409 (14) | 3643 (13) | 5.1 (4) |
| C(6) | 3087 (10) | 257 (15) | 3388 (14) | 5.6 (4) |
| C(7) | 3752 (14) | −428 (21) | 3411 (19) | 9.3 (6) |
| C(8) | 4392 (15) | 210 (24) | 3000 (20) | 10.7 (7) |
| C(9) | 2623 (9) | −702 (14) | 5514 (13) | 5.0 (4) |
| C(10) | 2382 (12) | −664 (19) | 6618 (17) | 8.1 (6) |
| C(11) | 3112 (18) | −984 (31) | 7458 (26) | 14 (1) |
| C(12) | 2841 (18) | −2033 (30) | 7322 (26) | 14 (1) |
| C(13) | 1955 (9) | 1010 (14) | 4969 (12) | 4.9 (3) |
| C(14) | 1463 (10) | 1619 (16) | 4199 (14) | 5.8 (4) |
| C(15) | 1383 (11) | 2861 (17) | 4490 (15) | 6.8 (5) |
| C(16) | 2071 (12) | 3528 (20) | 4417 (17) | 8.4 (6) |

[a] Tungsten and chlorine positional parameters have been multiplied by $10^5$; other positional parameters and all $U_{eq}$ by $10^4$.

**Table III.** Bond Lengths in $W_6Cl_{14}^{2-}$

| atom | atom | dist, Å | atom | atom | dist, Å |
|---|---|---|---|---|---|
| W(1) | W(2) | 2.610 (1) | Cl(2) | W(1) | 2.500 (4) |
| | W(3) | 2.611 (1) | | W(2) | 2.501 (4) |
| | W(2)′ | 2.602 (1) | | W(3) | 2.502 (4) |
| | W(3)′ | 2.603 (1) | | | |
| | | | Cl(3) | W(1) | 2.496 (3) |
| W(2) | W(3) | 2.607 (1) | | W(2) | 2.509 (3) |
| | W(3)′ | 2.607 (1) | | W(3) | 2.503 (3) |
| W(1) | W(1)′ | 3.686 (1) | Cl(4) | W(1) | 2.489 (3) |
| W(2) | W(2)′ | 3.685 (1) | | W(2) | 2.484 (3) |
| W(3) | W(3)′ | 3.688 (1) | | W(3) | 2.503 (3) |
| W(1) | Cl(7) | 2.419 (4) | Cl(5) | W(1) | 2.509 (4) |
| W(2) | Cl(1) | 2.413 (4) | | W(2) | 2.498 (4) |
| W(3) | Cl(6) | 2.416 (4) | | W(3) | 2.496 (4) |

and polarization corrections were applied. The data were merged to give 5572 independent reflections, of which 4410 had $F_o^2 > 0$ but only 1763 had $F_o^2 > 3\sigma F_o^2$. Variances were assigned in the same manner as above. The coordinates of the three independent tungsten atoms were obtained from a Patterson map. Subsequent structure factor–Fourier cycles gave the coordinates of the remaining non-hydrogen atoms. Several cycles of least-squares refinement with anisotropic thermal parameters for the tungsten and bromine atoms, isotropic thermal parameters for the nitrogen and carbon atoms in the cation, and a secondary extinction parameter converged with $R = 0.158$ for all the data with $F_o^2 > 0$ and 0.065 for the data with $F_o^2 > 3\sigma F_o^2$. The goodness of fit is 1.31 for $n = 5572$ reflections and $p = 160$ parameters. The maximum shift of any parameter in the final cycle was less than 25% of its standard deviation; the secondary extinction parameter was zero within its standard deviation. Final parameters are given in Table IV;[8] bond lengths and angles are given Table V.

**$[(n\text{-}C_4H_9)_4N]_2W_6I_{14}$.** A crystal with dimensions 0.33 × 0.24 × 0.29 mm was mounted on a glass fiber. Oscillation photographs of the crystal showed only one axis of symmetry, which characterizes monoclinic cells. The crystal was then centered on a Nicolet $P2_1$ diffractometer equipped with graphite-monochromated Mo Kα radiation for intensity data collection. Unit cell dimensions were obtained from the setting angles of 15 reflections with $25° < 2\theta < 28°$. Space group $P2_1/n$ was chosen on the basis of the systematic absences $h0l$, $h + l = 2n + 1$, and $0k0$, $k = 2n + 1$, in the intensity data. Two sets of data were collected with a total of 9860 reflections in the quadrants $h,k,\pm l$, and $h,-k,\pm l$. Crystal data are collected in Table I.

At every 97 reflections three check reflections were monitored to check crystal decay; they showed no variations greater than those expected

**Table IV.** Final Parameters for $[(n\text{-}C_4H_9)_4N]_2W_6Br_{14}$[a]

| atom | x | y | z | $U_{eq}$ or B, Å$^2$ |
|---|---|---|---|---|
| W(1) | 1812 (7) | −5729 (14) | −12780 (10) | 455 (4) |
| W(2) | 8434 (7) | −6099 (14) | 4897 (10) | 444 (4) |
| W(3) | 4680 (8) | 13167 (13) | −3395 (11) | 454 (4) |
| Br(1) | 11246 (18) | 12946 (36) | 14263 (26) | 568 (10) |
| Br(2) | −5518 (20) | 25022 (32) | 4591 (30) | 632 (10) |
| Br(3) | 14856 (17) | 1090 (34) | −11145 (25) | 613 (10) |
| Br(4) | −1950 (20) | 13499 (37) | −20946 (26) | 648 (11) |
| Br(5) | −20186 (18) | 14269 (36) | −11785 (31) | 735 (12) |
| Br(6) | −4184 (22) | 13220 (41) | 30729 (27) | 828 (13) |
| Br(7) | 11098 (21) | 31419 (36) | −8505 (32) | 826 (13) |
| N(1) | 2058 (14) | 244 (23) | 4783 (18) | 4.4 (6) |
| C(1) | 2347 (18) | 422 (30) | 3766 (24) | 5.0 (8) |
| C(2) | 3055 (29) | −127 (46) | 3513 (36) | 10 (1) |
| C(3) | 3647 (41) | 429 (61) | 3174 (48) | 16 (2) |
| C(4) | 4253 (31) | −231 (50) | 2840 (39) | 12 (2) |
| C(5) | 2582 (19) | 772 (31) | 5554 (26) | 5.8 (9) |
| C(6) | 2344 (29) | 735 (46) | 6604 (39) | 11 (2) |
| C(7) | 2909 (23) | 1517 (39) | 7172 (32) | 8 (1) |
| C(8) | 3327 (62) | 759 (99) | 7671 (32) | 34 (1) |
| C(9) | 1366 (24) | 856 (39) | 4923 (30) | 8 (1) |
| C(10) | 1364 (26) | 2168 (43) | 4780 (32) | 9 (1) |
| C(11) | 648 (30) | 2547 (51) | 5315 (37) | 11 (2) |
| C(12) | 688 (39) | 3739 (72) | 5280 (52) | 18 (3) |
| C(13) | 1912 (20) | −995 (34) | 5052 (27) | 6 (1) |
| C(14) | 1465 (18) | −1612 (31) | 4296 (24) | 5 (1) |
| C(15) | 1325 (24) | −2822 (40) | 4585 (30) | 8 (1) |
| C(16) | 1992 (26) | −3499 (41) | 4472 (33) | 9 (1) |

[a] Tungsten and bromine positional parameters have been multiplied by $10^5$; other positional parameters and all $U_{eq}$ by $10^4$.

**Table V.** Bond Lengths in $W_6Br_{14}^{2-}$

| atom | atom | dist, Å | atom | atom | dist, Å |
|---|---|---|---|---|---|
| W(1) | W(2) | 2.643 (2) | Br(1) | W(1) | 2.626 (4) |
| | W(3) | 2.625 (2) | | W(2) | 2.637 (4) |
| | W(2)′ | 2.630 (2) | | W(3) | 2.638 (4) |
| | W(3)′ | 2.643 (2) | | | |
| | | | Br(2) | W(1) | 2.633 (4) |
| W(2) | W(3) | 2.638 (2) | | W(2) | 2.636 (4) |
| | W(3)′ | 2.631 (2) | | W(3) | 2.631 (4) |
| W(1) | W(1)′ | 3.728 (2) | Br(3) | W(1) | 2.610 (4) |
| W(2) | W(2)′ | 3.729 (2) | | W(2) | 2.612 (4) |
| W(3) | W(3)′ | 3.722 (2) | | W(3) | 2.629 (4) |
| W(1) | Br(6) | 2.588 (4) | Br(4) | W(1) | 2.628 (4) |
| W(2) | Br(5) | 2.586 (4) | | W(2) | 2.627 (4) |
| W(3) | Br(7) | 2.587 (4) | | W(3) | 2.629 (4) |

statistically. The data were corrected for absorption by Gaussian integration over an 8 × 8 × 8 grid; transmission factors varied from 0.107 to 0.212. After being corrected for background, the two data sets were merged to give 4269 independent reflections, which were all used in the structure solution and refinement. Variances were assigned to the individual reflections in the same manner as described above.

The anions are located at a center of symmetry in the unit cell. Interpretation of Patterson maps gave the positions of the three tungsten atoms. From structure factor–Fourier calculations the seven iodine atoms and the non-hydrogen atoms in the cation were located. The positions of the hydrogen atoms were calculated from known geometry and assumed staggered conformations. The tungsten and iodine atoms were given anisotropic thermal parameters while the atoms in the cation were given isotropic thermal parameters. Several cycles of least-squares refinement led to convergence with $R$ of 0.090 for 3463 data with $F_o^2 > 3\sigma F_o^2$. The goodness of fit (defined above) is 2.23 for $n = 4260$ reflections and $p = 167$ parameters (nine strong, low-angle reflections were given zero weight in the refinement). Final parameters are given in Table VI,[8] and bond lengths are listed in Table VII.

The cations are not well-behaved in the refinements,[9] but this has no effect on the W or X parameters. During the least-squares refinement, the carbon positions were allowed to vary freely. In the $[(n\text{-}C_4H_9)_4N]_2W_6Cl_{14}$ structure, for example, the C–N bond distances vary from 1.488 to 1.535 Å and the C–C bond distances from 1.292 to 1.540 Å. The tetrahedral angles vary from 108.3 to 117.9°. Final three-dimensional difference maps calculated for all three structures showed no

(9) The refinements in all three cations led to large values of $B$ and unrealistic C–C distances.

**Table VI.** Final Parameters for $[(n\text{-}C_4H_9)_4N]_2W_6I_{14}$[a]

| atom | x | y | z | $U_{eq}$ or B, Å$^2$ |
|---|---|---|---|---|
| W(1) | 4454 (1) | 4328 (1) | 5624 (1) | 597 (4) |
| W(2) | 6475 (1) | 4300 (1) | 5191 (1) | 602 (4) |
| W(3) | 4497 (1) | 3673 (1) | 4587 (1) | 622 (4) |
| I(1) | 3634 (2) | 3344 (2) | 6568 (1) | 967 (8) |
| I(2) | 8693 (2) | 3233 (2) | 5464 (1) | 1011 (8) |
| I(3) | 3794 (3) | 1692 (2) | 3950 (1) | 1135 (9) |
| I(4) | 3502 (2) | 5039 (2) | 3714 (1) | 778 (6) |
| I(5) | 5443 (2) | 2188 (2) | 5424 (1) | 800 (6) |
| I(6) | 6586 (2) | 3584 (2) | 4112 (1) | 839 (7) |
| I(7) | 2361 (2) | 3661 (2) | 5022 (1) | 747 (6) |
| N(1) | 5154 (25) | 4758 (23) | 1675 (9) | 6.3 (6) |
| C(1) | 3815 (37) | 4479 (32) | 1600 (14) | 8 (1) |
| C(2) | 3201 (36) | 4665 (31) | 2148 (13) | 7.5 (9) |
| C(3) | 2080 (47) | 4058 (44) | 2126 (16) | 10 (1) |
| C(4) | 2036 (50) | 2911 (46) | 2176 (18) | 12 (1) |
| C(5) | 5577 (35) | 4546 (29) | 1094 (13) | 7.0 (8) |
| C(6) | 6822 (41) | 4875 (37) | 1079 (15) | 9 (1) |
| C(7) | 6979 (98) | 4604 (87) | 485 (44) | 10 (3) |
| C(8) | 7872 (86) | 5164 (79) | 299 (33) | 7 (2) |
| C(9) | 5813 (33) | 3962 (31) | 2160 (12) | 6.7 (8) |
| C(10) | 5584 (33) | 2690 (29) | 2092 (12) | 6.5 (8) |
| C(11) | 6087 (37) | 2208 (32) | 2613 (14) | 7.9 (9) |
| C(12) | 5890 (46) | 840 (40) | 2587 (16) | 11 (1) |
| C(13) | 5438 (30) | 6015 (26) | 1866 (11) | 5.6 (7) |
| C(14) | 4985 (37) | 6940 (34) | 1453 (14) | 8 (1) |
| C(15) | 5474 (38) | 8178 (34) | 1654 (14) | 8.1 (9) |
| C(16) | 5139 (40) | 9105 (35) | 1261 (15) | 9 (1) |

[a] Positional parameters and $U_{eq}$ have been multiplied by $10^4$.

**Table VII.** Bond Lengths in $W_6I_{14}^{2-}$

| atom | atom | dist, Å | atom | atom | dist, Å |
|---|---|---|---|---|---|
| W(1) | W(2) | 2.676 (2) | I(4) | W(1) | 2.800 (2) |
| | W(3) | 2.661 (2) | | W(2) | 2.790 (2) |
| | W(2)′ | 2.671 (2) | | W(3) | 2.792 (2) |
| | W(3)′ | 2.674 (2) | | | |
| | | | I(5) | W(1) | 2.778 (3) |
| W(2) | W(3) | 2.673 (2) | | W(2) | 2.792 (3) |
| | W(3)′ | 2.668 (2) | | W(3) | 2.792 (3) |
| W(1) | W(1)′ | 3.777 (2) | I(6) | W(1) | 2.792 (3) |
| W(2) | W(2)′ | 3.785 (2) | | W(2) | 2.792 (3) |
| W(3) | W(3)′ | 3.768 (2) | | W(3) | 2.803 (3) |
| W(1) | I(1) | 2.842 (3) | I(7) | W(1) | 2.788 (2) |
| W(2) | I(2) | 2.849 (3) | | W(2) | 2.780 (2) |
| W(3) | I(3) | 2.826 (3) | | W(3) | 2.802 (2) |

features other than some peaks close to the heavy-atom positions of 2 or 3 e Å$^{-3}$, typical residuals for structures such as these.

## Results and Discussion

Although octahedral symmetry is not imposed crystallographically, all three clusters have nearly perfect octahedra of tungsten atoms. An ORTEP drawing of the unit cell of $[(n\text{-}C_4H_9)_4N]_2W_6Br_{14}$ is shown in Figure 1. The octahedra expand in the (W–W bond length) order $W_6Cl_{14}^{2-} < W_6Br_{14}^{2-} < W_6I_{14}^{2-}$ (Table VIII). If the emissive excited states in the tungsten clusters were completely metal-centered, as appears to be the case in the molybdenum series,[2] their energies should correspond to the lengths of the metal–metal bonds. One would expect that the shorter the metal–metal bond, the greater the overlap of the metal d orbitals and, therefore, the higher the energy of the emissive state.[4] But in the tungsten clusters we observe the opposite trend, and thus we conclude that the energies of the excited states for the clusters are not determined by the tungsten–tungsten bond distances.[10]

(10) The assumption is that the Mo–Mo distances in the clusters $Mo_6X_{14}^{2-}$ are constant, since the emissive excited states are isoenergetic. Unfortunately, only the structure of the $Mo_6Cl_{14}^{2-}$ ion has been reported (Vaughn, P. A. *Proc. Natl. Acad. Sci. U.S.A.* **1950**, *36*, 461), so this is conjecture. We have completed the structure of the one-electron-oxidized $(PPN)W_6Br_{14}$ cluster and found that the structure is similar to those reported here, with *d*(W–X(axial)) shorter than in the 2– anion, as expected from the greater electrostatic attraction (Zietlow, T. C.; Schaefer, W. P.; Sadeghi, B.; Nocera, D. G.; Gray, H. B. *Inorg. Chem.*, following paper in this issue.

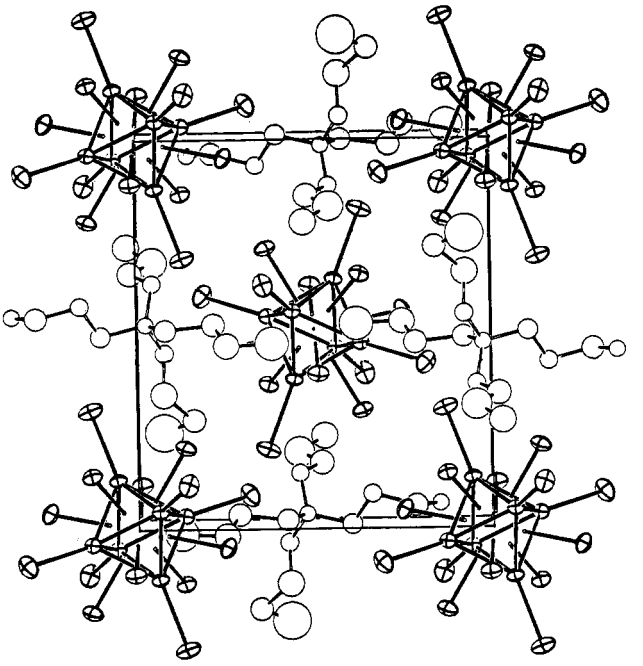

**Figure 1.** ORTEP view of the $(TBA)_2W_6Br_{14}$ structure, approximately down *a*, with the unit cell outlined (30% probability thermal ellipsoids shown).

**Table VIII.** Average Bond Distances (Å)

| bond | $W_6Cl_{14}^{2-}$ | $W_6Br_{14}^{2-}$ | $W_6I_{14}^{2-}$ |
|---|---|---|---|
| W–W(cis) | 2.607 (4) | 2.635 (7) | 2.671 (5) |
| W–W(trans) | 3.686 (2) | 3.726 (4) | 3.777 (9) |
| W–X(facial) | 2.499 (7) | 2.628 (9) | 2.792 (7) |
| W–X(axial) | 2.416 (3) | 2.587 (1) | 2.839 (1) |
| X(facial)–X(axial) | 3.530 (32) | 3.692 (34) | 3.920 (28) |

Can we find any correlations with the tungsten–halide bond distances (Table VIII)? In the tungsten chloride cluster, the tungsten–chloride (axial) bond is shorter than the tungsten–chloride (facial) bond. In the tungsten bromide cluster, the bond lengths are nearly the same; there is a significantly smaller difference relative to the analogous tungsten–chloride bonds. And in the tungsten iodide structure, the tungsten–iodide (axial) bond is longer than the tungsten–iodide (facial) bond. There appears to be a stronger bonding interaction of the tungsten atom with the $\mu_3$-iodide ligand than with the $\mu_3$-chloride in the $W_6Cl_{14}^{2-}$ cluster. The $WX_4$ units in all three structures are planar within the error limits of the data, so the W–X(facial) distance is the important parameter in assessing the relative strength of the interaction.

This systematic change is manifested in the changes in the emission spectra as a function of axial halide. In the $W_6Cl_8^{4+}$ core, the emission bands shift over 400 cm$^{-1}$ upon exchange of the axial halides from chloride to iodide. With the $W_6I_8^{4+}$ core, this shift is only about 60 cm$^{-1}$.[5] Clearly, the axial halides exhibit stronger interactions with the metal framework in $W_6Cl_8^{4+}$ than in $W_6I_8^{4+}$, in accord with the crystallographic findings. The longer $W\text{–}X_a$ distances in the bromide and iodide structures (after accounting for the ionic radii differences) may be due in part to steric replusions from the facial halides.

While the exact nature of the emissive states of the $W_6X_{14}^{2-}$ clusters is not known, calculations[2,4] as well as experimental data[5] indicate that the tungsten $d_{xy}$ atomic orbitals are important in describing their electronic structures. It is likely, for example, that the excited-state energies of the $W_6X_{14}^{2-}$ species are influenced by the strengths of $\pi$ interactions involving the bridging halides and $d_{xy}$ combinations. On the basis of standard $\pi$-donor considerations, iodides would be expected to decrease the energy gap between the HOMO and LUMO of the clusters, thereby leading to a lower energy emissive state. Since this is not observed experimentally, ligand $\pi$-donation must not be the factor that determines the excited-state energy.

The unusually favorable interactions of the facial iodides with the tungsten atoms imply that there is metal cluster back-bonding to the ligands, using empty d orbitals on iodide to accept electron density from the electron-rich tungsten(II) unit. The emission energy ordering can be explained in this way, since iodide should be a better $\pi$-acceptor than chloride; d-d $\pi$-bonding would lower the energy of the HOMO, resulting in a larger energy gap for the tungsten iodide cluster.

**Acknowledgment.** We thank Miriam Heinrichs, Mike Hopkins, and Dan Nocera for many helpful discussions. T.C.Z. acknowledges a graduate fellowship from the Sun Co. This research was supported by National Science Foundation Grants CHE84-19828 (H.B.G.), CHE82-19039 (X-ray facility), and the Exxon Educational Foundation (W.P.S., B.S.).

**Registry No.** $[(n\text{-}C_4H_9)_4N]_2W_6Cl_{14}$, 84648-02-2; $[(n\text{-}C_4H_9)_4N]_2W_6Br_{14}$, 96390-92-0; $[(n\text{-}C_4H_9)_4N]_2W_6I_{14}$, 27680-20-2.

**Supplementary Material Available:** Tables of stucture factors and anisotropic thermal parameters for the refined atoms (61 pages). Ordering information is given on any current masthead page.

---

Contribution No. 7216 from the Arthur Amos Noyes Laboratory, California Institute of Technology, Pasadena, California 91125

# Preparation and Properties of $[((C_6H_5)_3P)_2N]W_6Br_{14}$

Thomas C. Zietlow, William P. Schaefer, Behzad Sadeghi, Daniel G. Nocera, and Harry B. Gray*

*Received June 26, 1985*

$(PPN)W_6Br_{14}$ [PPN = $((C_6H_5)_3P)_2N^+$] was prepared by the reaction of $(PPN)_2W_6Br_{14}$ and $NOPF_6$ in degassed methylene chloride solution. $(PPN)W_6Br_{14}$ crystallizes in the monoclinic space group $P2_1/n$ with $a$ = 9.577 (2) Å, $b$ = 22.478 (6) Å, $c$ = 24.430 (4) Å, $\beta$ = 97.42 (2)°, and $Z$ = 4. The tungsten-tungsten bonds are longer in $W_6Br_{14}^-$ than in $W_6Br_{14}^{2-}$ [$d$(W-W): $W_6Br_{14}^-$ = 2.649 (8) Å; $W_6Br_{14}^{2-}$ = 2.635 (7) Å], consistent with the electron being removed from a metal-metal bonding orbital. The metal-bromide bonds are shorter in the monoanion than in the dianion [$d$(W-Br(axial)): $W_6Br_{14}^-$ = 2.538 (12) Å; $W_6Br_{14}^{2-}$ = 2.587 (4) Å], probably due to the greater electrostatic attraction of the halide to the oxidized metal cluster. The electronic absorption spectra of $W_6Br_{14}^-$ and related cluster monoanions indicate that the lowest energy allowed transition [551 nm ($\epsilon$ = 2560 $M^{-1}$ $cm^{-1}$) for $W_6Br_{14}^-$ in $CH_2Cl_2$] is ligand-to-metal charge transfer from an axial halide. The magnetic properties (EPR, magnetic susceptibility) of $(PPN)W_6Br_{14}$ are consistent with a $^2E$ ground state.

The nature of the structural distortion in the emissive excited states of the $M_6X_{14}^{2-}$ (M = Mo, W; X = Cl, Br, I) clusters is not known.[1] Because it is likely that this excited state has one electron removed from the $M_6X_{14}^{2-}$ highest occupied molecular orbital,[1c] the one-electron-oxidized clusters ($M_6X_{14}^-$) should reveal at least certain aspects of the distortion in the emissive species. Accordingly, we have performed a crystal structure analysis of one of the oxidized compounds, $(PPN)W_6Br_{14}$ [PPN = $((C_6H_5)_3P)_2N^+$], which is reported here along with the electronic absorption spectra of several oxidized tungsten cluster complexes. Additional information about the electronic structure of $(PPN)W_6Br_{14}$ has been extracted from a 9 K EPR spectrum and variable-temperature magnetic susceptibility measurements.

## Experimental Section

Optical absorption spectra were recorded on a Cary 17 spectrometer. Electron paramagnetic resonance spectra were measured on a Varian E-Line Century Series spectrometer equipped with an Air-Products Heli-Tran cooling system. Variable-temperature susceptibility measurements were made at the University of Southern California on a SQUID-based (SHE Corp.) Model 805 variable-temperature susceptometer with a 2 K option.

**$(PPN)_2W_6Br_{14}$** was synthesized by mixing $W_6Cl_{12}$ (0.50 g) in an evacuated tube with a 20-fold excess of LiBr:KBr (40:60 mixture) (3.07 g:2.86 g) and heating the sealed tube at 360 °C for 30 min. After cooling, the tube was broken and the contents dissolved in 6 M HBr. This solution was treated with (PPN)Cl, causing a precipitate to form; the solid material was filtered off, dried in vacuo, and recrystallized from methylene chloride/petroleum ether.

**$(PPN)W_6Br_{14}$** was synthesized by reacting $(PPN)_2W_6Br_{14}$ with $NOPF_6$ in degassed methylene chloride solution. Crystallization of the product by layering with petroleum ether resulted in deep red crystals. (A few yellow crystals of starting material also were obtained; these were carefully dissolved off with acetonitrile.) Anal. Calcd for $C_{36}H_{30}P_2NW_6Br_{14}$: C, 15.55; H, 1.10; N, 0.51. Found: C, 16.14; H, 1.17; N, 0.51.

**Table I.** Crystal Data for $[Ph_3P{=}N{=}PPh_3][W_6Br_{14}]$

| | |
|---|---|
| formula: $W_6Br_{14}P_2NC_{36}H_{30}$ | $F(000)$ = 4868 e |
| $a$ = 9.577 (5) Å | fw = 2760.43 |
| $b$ = 22.478 (12) Å | space group: $P2_1/n$ (No. 14) |
| $c$ = 24.430 (8) Å | $T$ = 21 °C |
| $\beta$ = 97.42 (2)° | $\lambda$(Mo K$\alpha$) = 0.71073 Å |
| $V$ = 5215 (6) Å$^3$ | $d_{exptl}$ = 3.47 g cm$^{-3}$ |
| $\mu$ = 253.5 cm$^{-1}$ | |

**$(TBA)W_6Cl_{14}$, $(TBA)W_6Cl_8Br_6$, and $(TBA)W_6Br_8Cl_6$** [TBA = $(C_4H_9)_4N^+$] were generated by $NOPF_6$ oxidation of the corresponding cluster dianions in degassed methylene chloride solution.[2]

**X-ray Structure Determination.** A crystal 0.23 × 0.28 × 0.20 mm with faces {011} and (10$\bar{1}$), ($\bar{1}$01) was chosen. Preliminary photographs showed a monoclinic cell; the crystal was transferred to a Nicolet $P2_1$ diffractometer equipped with graphite-monochromated Mo K$\alpha$ radiation, and unit cell dimensions were obtained from the setting angles of 15 reflections with $20° < 2\theta < 30°$. Crystal data are given in Table I. Systematic absences in the diffractometer data of $h0l$, $h + l = 2n + 1$, and $0k0$, $k = 2n + 1$, indicate space group $P2_1/n$, a special setting of No. 14, with equivalent positions $\pm(x, y, z; {}^1/_2 - x, {}^1/_2 + y, {}^1/_2 - z)$. A total of 11 670 reflections with $2\theta < 40°$ in quadrants $h,k,\pm l$ and $h,-k,\pm l$ were measured with $\omega$ scans 1° wide at 1°/min. Three check reflections were monitored every 97 reflections and showed no variations greater than those expected statistically. The data were corrected for absorption by Gaussian integration over an 8 × 8 × 8 grid (transmission factors ranged from 0.013 to 0.044) and Lorentz and polarization factors were applied. The data were merged to give 4875 independent reflections, all of which were used in the structure solution and refinement; the goodness of fit

(1) (a) Maverick, A. W.; Gray, H. B. *J. Am. Chem. Soc.* **1981**, *103*, 1298. (b) Maverick, A. W.; Najdzionek, J. S.; MacKenzie, D.; Nocera, D. G.; Gray, H. B. *J. Am. Chem. Soc.* **1983**, *105*, 1878. (c) Zietlow, T. C.; Hopkins, M. D.; Gray, H. B. *J. Solid State Chem.* **1985**, *57*, 112.

(2) The initial products of oxidation of the other $(TBA)_2W_6X_8Y_6$ clusters decomposed at room temperature in dichloromethane solution as evidenced by changing electronic absorption spectral features with time. The reported data are for spectra that did not change over several days in solution.

0020-1669/86/1325-2198$01.50/0 